

Garment Texture Completion in UV space using Stable Diffusion

Ludek Cizinsky

ludek.cizinsky@epfl.ch yingxuan.you@epfl.ch

EPFL

Yingxuan You*

EPFL

Abstract

We present a method for completing garment texture maps in UV space using a diffusion model conditioned on masked input and text prompts. Our approach focuses on predicting diffuse textures as a first step toward high-fidelity, physically based rendering (PBR) of garments. To train our model, we construct a synthetic dataset of 27,000 garment textures with corresponding PBR maps generated using the DressCode pipeline. We fine-tune a Stable Diffusion v1.5 model and systematically evaluate the impact of guidance scale, training strategy, and dataset size. Our findings show that image guidance plays a critical role, and surprisingly strong performance can be achieved even with a small subset of training data. The proposed method significantly outperforms non-finetuned baselines on LPIPS, SSIM, and PSNR metrics. We provide an in-depth analysis of failure cases and outline key directions for future work.

1 Introduction

There is an increasing interest in digitalising garments, that is, converting an image of a person wearing clothing into a 3D model of the depicted garments. In this work, we focus specifically on extracting high-quality physically based rendering (PBR) texture maps. In particular, we target three key components: diffuse, which captures the base color of the garment material; normal, which represents the surface orientation; and roughness, which characterizes the smoothness or roughness of the surface.

PBR texture maps are essential for realistic rendering of garment appearance and are thus of particu-

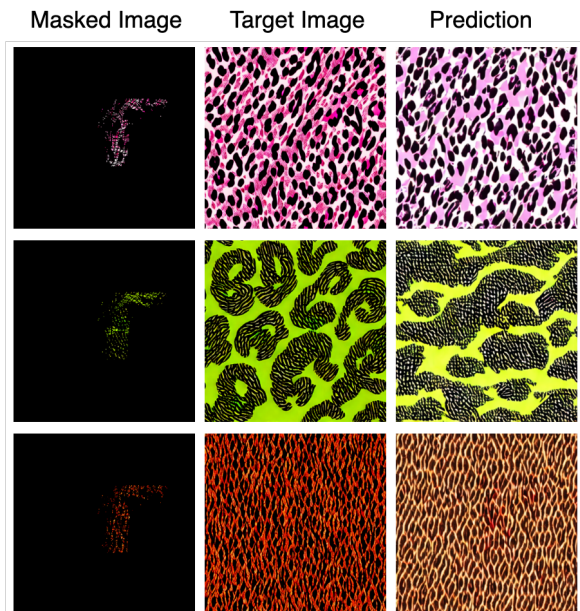


Figure 1. **Example of Diffuse Texture Predictions.** The model predicts the diffuse texture based on the observed partial masked image.

lar importance for downstream applications in gaming and the film industry. However, most existing methods extract only RGB texture maps, which include baked-in lighting from the original environment, limiting their adaptability and usefulness for other scenes or renderers.

Extracting high-quality PBR texture maps from a single RGB image poses several challenges. First, the problem involves modeling both the geometry and the appearance of the garment. Input images typically vary in lighting conditions and camera positions, making it difficult to disentangle material properties from illumination. In addition, garments themselves introduce domain-specific complications: self-occlusions often obscure parts of the fabric, which hinders accurate pattern capture; logos may be difficult to isolate and are frequently overlaid on the fabric in ways that complicate extraction; and finally, garment textures exhibit significant vari-

*Yingxuan contributed the initial research idea and the foundational model pipeline, building on her prior work. Throughout the semester, she provided Ludek with valuable guidance and constructive feedback.

ation, ranging from simple, repetitive motifs to complex, irregular patterns.

Most prior work has concentrated on the geometry, while texture modeling is usually simplified to generating *RGB* texture maps, as seen in methods such as *Garment3DGen* Sarafianos et al. (2025), *Deep-Iron* Kwon and Lee (2023), or *Wardrobe* Srivastava et al. (2024). To the best of our knowledge, *Fabric Diffusion* (FBD) Zhang et al. (2024a) is the only method that directly attempts to generate PBR texture maps from a single image. However, this approach comes with limitations. FBD relies on a user-provided patch of the garment to model local texture patterns, assuming these can be seamlessly tiled to cover the surface. This assumption fails when patterns are not globally repetitive, and it may produce unnatural seams between tiles. Additionally, logo extraction in FBD requires the user to manually crop the logo, after which the model removes background and lighting artifacts. While effective in isolated cases, this process is impractical for full-garment digitalisation and does not generalise well to garments with multiple logos.

A further bottleneck in this field is the absence of a large-scale public dataset that pairs garment images with corresponding PBR texture maps. This data gap presents a key obstacle to training more robust and generalisable models for PBR texture extraction from images.

In this work, we take a first step toward scalable, fully-automated garment digitalization by addressing the task of UV-space texture inpainting. Given a partially observed diffuse texture map, our goal is to complete the garment appearance in UV space, and predict corresponding diffuse (Figure 1), normal and roughness texture maps. For simplicity, we do not address logo modeling.

To inform our method design, we conduct a systematic evaluation of key training and inference choices. We ask: (1) What are the optimal text and image guidance scales during inference? (2) What is the best initialization strategy for fine-tuning? (3) How do training set size and duration affect model performance?

We find that a text guidance scale of 1.5 and image scale of 5.0 yield the best results. Further, initializing from InstructPix2Pix and fine tuning the full model leads to the best performance. Surprisingly,

we observe that training on only 5k images performs nearly as well as using the full 27k set, although longer training time consistently improves results.

We summarise our contributions as follows:

- We introduce a new dataset of 27,000 PBR texture maps generated by a pre-trained Dress-Code He et al. (2024) model.
- We propose a new method for UV-space texture inpainting that is trained on the proposed dataset.
- We conduct a systematic evaluation of key training and inference choices.
- We show that our method achieves the best performance on all metrics compare to the existing state-of-the-art inpainting methods.

All the code and data is available via the following link: <https://bit.ly/garment-diffusion>.

2 Related Work

General Material Texture Generation. *Tex-Gen* Yu et al. (2024) proposes a generative model for RGB texture synthesis in UV space, conditioned on either image or text inputs, and integrates 3D geometry information into the texture generation pipeline. *Material Palette* Lopes et al. (2024) targets PBR material extraction from single images of real-world surfaces and introduces LoRA-based fine-tuning of diffusion models. *DreamPBR* Xin et al. (2024) and *DreamMat* Zhang et al. (2024b) explore high-quality PBR texture generation from text, with the former supporting multi-modal inputs including fabric-related prompts. However, their models are either unpublished or lack garment-specific outputs such as normal maps. *MatFusion* Sartor and Peers (2023) addresses the removal of baked-in lighting from input images for SVBRDF estimation and serves as a key component in *FabricDiffusion*'s PBR extraction pipeline. Our work draws inspiration from these (e.g. considering using LoRA for finetuning) advances while focusing specifically on garment texture reconstruction.

Garment Texture Generation. *FabricDiffusion* Zhang et al. (2024a) proposes a two-stage pipeline that first normalizes RGB garment textures and then employs an external model to predict the corresponding PBR texture maps, lever-

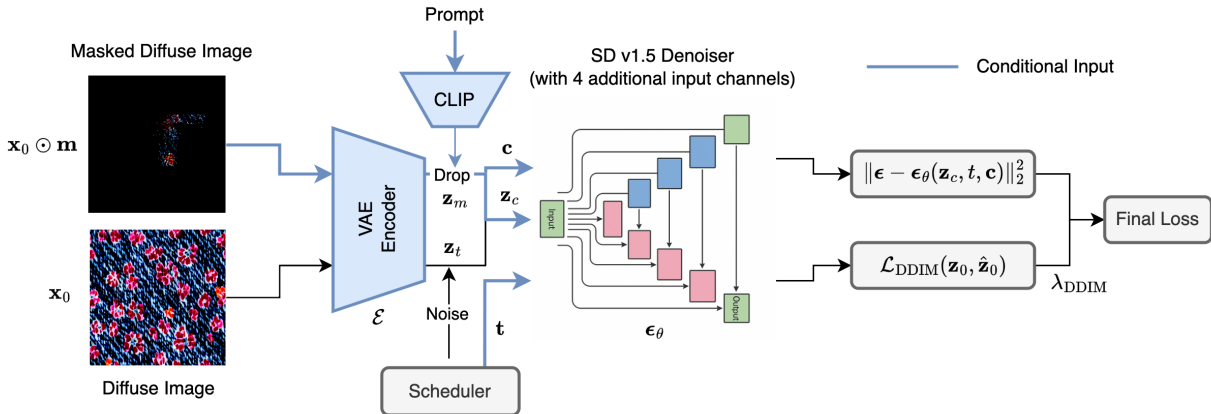


Figure 2. Overview of the Training Pipeline. Inputs are first encoded into the latent space using a pre-trained (frozen) VAE and CLIP encoder. A timestep t is sampled via the PNDM scheduler, and noise is added to the target image latent. The diffusion model is conditioned on the noisy latent, masked image latent, timestep, and text prompt. It is trained to predict the added noise, with supervision from a weighted sum of MSE and DDIM reconstruction losses.

aging prior SVBRDF estimation techniques. *Garment3DGen* Sarafianos et al. (2025) introduces a multi-stage framework for 3D garment modeling, combining geometry and texture streams into a renderable output; however, it relies solely on RGB textures. Similarly, *DeepIron* Kwon and Lee (2023) presents a pipeline involving garment segmentation, texture unwrapping, and inpainting, followed by application of the recovered texture onto a predefined sewing pattern, with its main novelty being the learned unwarping module. Our approach differs in focusing explicitly on recovering garment-specific diffuse texture maps for the entire garment (not just a patch like in *FabricDiffusion*).

3D Garment Generation. *DressCode* He et al. (2024) introduces a multi-stage framework for text-driven garment synthesis, combining an autoregressive model that generates sewing patterns from prompts with a conditional diffusion model that produces corresponding PBR textures. *WordRobe* Srivastava et al. (2024) maps text inputs to textured 3D garments via a disentangled latent garment space and CLIP-based alignment, but produces only RGB textures. *Design2Cloth* Zheng et al. (2024) enables mask-guided 3D garment generation and releases a large dataset of over 27,000 real-world garment scans. *PICTURE* Ning et al. (2024) offers greater design flexibility by disentangling garment style and texture, employing a two-stage pipeline

that first predicts garment shape and then generates texture conditioned on that shape. Finally, *VTON360* He et al. (2025) addresses the challenge of viewpoint consistency in virtual try-on, introducing a method for generating high-fidelity garments renderable from arbitrary angles. All these approaches focus on end-to-end 3D garment generation. In contrast, our method focuses specifically on high-quality *texture reconstruction* from real images, aiming to recover physically meaningful material properties. As such, it can serve as a plug-in module for enhancing the realism and generalizability of generative pipelines that rely on RGB textures or simplified appearance models.

3 Method

Latent Diffusion Model. We make use of a pre-trained VAE Kingma and Welling (2022) encoder-decoder pair $(\mathcal{E}, \mathcal{D})$ for diffuse textures, where $\mathcal{E} : \mathbb{R}^{H \times W \times 3} \rightarrow \mathbb{R}^{C \times H' \times W'}$ encodes RGB images into a latent space, and \mathcal{D} maps latents back to image space. The decoder was specifically fine-tuned for the task of reconstructing diffuse textures He et al. (2024).

Figure 2 shows an overview of our fine tuning pipeline. Given an input diffuse texture x_0 and a binary mask m , we encode the full and masked tex-

Model	LPIPS ↓	SSIM ↑	PSNR ↑
Ours	0.45	0.17	13.04
Kandinsky 2.2	0.91	0.09	9.55
SD-Inpaint	0.97	0.02	6.56
Pix2Pix	1.00	0.03	6.36
SD	0.95	0.02	6.46

(a) Comparison to non-finetuned baselines.

TNS	TT [hrs]	LPIPS ↓	SSIM ↑	PSNR ↑
27,000	30	0.50	0.16	12.41
27,000	60	0.45	0.17	13.04
5,000	30	0.49	0.17	13.11
15,000	30	0.50	0.16	13.10
20,000	30	0.51	0.17	13.12
10,000	30	0.52	0.17	12.65

(b) Effect of training set size and training time.

Table 1. **Comparison to Non-Finetuned Baselines and Scale Study.**

tures using the VAE encoder:

$$\mathbf{z}_0 = \mathcal{E}(\mathbf{x}_0), \quad \mathbf{z}_m = \mathcal{E}(\mathbf{x}_0 \odot \mathbf{m}), \quad (1)$$

where \odot denotes element-wise multiplication. We then sample a timestep $t \sim \mathcal{U}(1, T)$, using PNDM scheduler Liu et al. (2022), and generate a noisy latent:

$$\mathbf{z}_t = \sqrt{\bar{\alpha}_t} \mathbf{z}_0 + \sqrt{1 - \bar{\alpha}_t} \boldsymbol{\epsilon}, \quad \boldsymbol{\epsilon} \sim \mathcal{N}(0, \mathbf{I}), \quad (2)$$

where $\bar{\alpha}_t$ is the cumulative product of noise schedule coefficients. We then concatenate the masked latent \mathbf{z}_m and the noisy latent \mathbf{z}_t to form the input to the diffusion model:

$$\mathbf{z}_c = [\mathbf{z}_m, \mathbf{z}_t] \quad (3)$$

A conditioning text prompt \mathbf{c} (constant across all samples) is embedded using CLIP Radford et al. (2021). To enable classifier-free guidance Ho and Salimans (2022), we randomly drop the conditioning with some probability p_{drop} .

The model $\boldsymbol{\epsilon}_{\theta}$ is trained to predict the noise $\boldsymbol{\epsilon}$ added to \mathbf{z}_0 . The total loss is then a weighted sum of the denoising objective and a DDIM reconstruction loss:

$$\begin{aligned} \mathcal{L} &= \|\boldsymbol{\epsilon} - \boldsymbol{\epsilon}_{\theta}(\mathbf{z}_c, t, \mathbf{c})\|_2^2 \\ &+ \lambda_{\text{DDIM}} \cdot \mathcal{L}_{\text{DDIM}}(\mathbf{z}_0, \hat{\mathbf{z}}_0) \end{aligned} \quad (4)$$

where $\hat{\mathbf{z}}_0$ is the model’s reconstruction using DDIM inversion Song et al. (2022) and λ_{DDIM} is the weight of DDIM loss.

During inference, we adopt the same approach as in *InstructPix2Pix* Brooks et al. (2023), where we condition the diffusion model on latents of the masked texture \mathbf{z}_m and text prompt \mathbf{z}_c to iteratively denoise

from the noisy input image \mathbf{z}_T to $\hat{\mathbf{z}}_0$. Importantly, we make use of classifier-free guidance Ho and Salimans (2022) to enable control over the text prompt and image guidance influence on the final texture. Based on our experiments, we find the text guidance scale $w_T = 1.5$ and image guidance scale $w_I = 5.0$ to be optimal. Using these guidance scales, we can express the classifier-free guidance as:

$$\begin{aligned} \tilde{\boldsymbol{\epsilon}}_{\theta}(\mathbf{z}_t, \mathbf{c}_I, \mathbf{c}_T) &= \boldsymbol{\epsilon}_{\theta}(\mathbf{z}_t, \emptyset, \emptyset) \\ &+ w_I \cdot (\boldsymbol{\epsilon}_{\theta}(\mathbf{z}_t, \mathbf{c}_I, \emptyset) - \boldsymbol{\epsilon}_{\theta}(\mathbf{z}_t, \emptyset, \emptyset)) \\ &+ w_T \cdot (\boldsymbol{\epsilon}_{\theta}(\mathbf{z}_t, \mathbf{c}_I, \mathbf{c}_T) - \boldsymbol{\epsilon}_{\theta}(\mathbf{z}_t, \mathbf{c}_I, \emptyset)) \end{aligned} \quad (5)$$

Finally, to map the predicted latent back to image space, we make use of texture specific pretrained decoder \mathcal{D} adapted from *DressCode* He et al. (2024).

Data. We generate a dataset of 27,000 PBR texture maps using pretrained DressCode He et al. (2024) model. Specifically, we first generate 30 different queries for colour, texture and pattern. We then feed each possible combination of these queries to the DressCode model which then generates a corresponding PBR texture map.

4 Results

4.1 Experimental Setup

Our best model is trained on a single NVIDIA V100 GPU for 60 hours using a batch size of 20. We optimize using the AdamW optimizer with a learning rate of 1×10^{-4} , a weight decay of 1×10^{-2} , and 1000 warm-up steps. To stabilize training, we apply gradient clipping based on the ℓ_2 -norm. Input images are used at their original resolution of 512×512 pixels. The DDIM loss is scaled by a factor of 0.5. Training is performed on the full dataset comprising

DDIM Weight	LR	BSZ	LoRA	Scratch	Inpaint	Base Model	LPIPS ↓	SSIM ↑	PSNR ↑
0.50	1e-04	20	\times	\times	\times	sd	0.50	0.16	12.41
0.50	1e-04	40	✓	\times	\times	pix2pix	0.57	0.09	11.75
0.50	1e-05	20	\times	✓	\times	sd	0.82	0.02	7.48
0.75	1e-04	20	✓	\times	✓	sd-inpaint	0.96	0.13	9.25

Table 2. **Ablation Study Over Model Architecture and Training Strategy.** All models trained for 30 hours on 27,000 samples. Best results per metric are highlighted in bold. Top row shows the best model for reference.

Text Scale	Image Scale	LPIPS Rank	SSIM Rank	PSNR Rank	Mean Rank
5.0	2.5	6.0	7.0	5.0	6.00
1.5	5.0	9.0	4.0	6.0	6.33
2.5	7.5	10.0	2.0	9.0	7.00

Table 3. **Guidance Scale Ranking.** The best performing configuration is highlighted in bold. The table shows the rank of each configuration on SSIM, PSNR, and LPIPS.

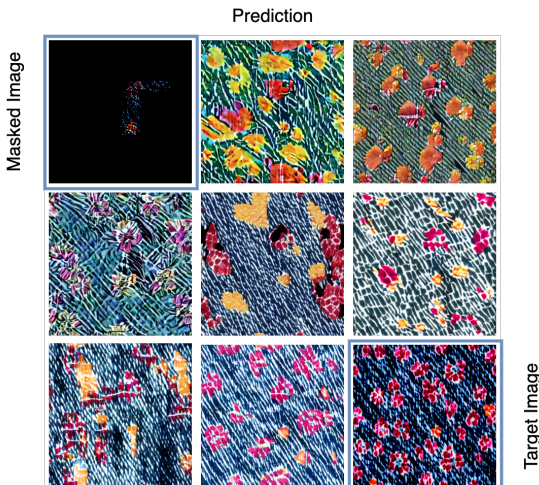


Figure 3. **Evolution of the Best Model’s Predictions.** The model’s predictions on a single validation sample over the training process. First prediction in the figure made after 10,000 steps. The following predictions are made every 5,000 steps.

ing 27,000 samples, with validation conducted every 1000 steps on a held-out set of 300 images. During inference, we employ a guidance scale of 1.5 for text and 5.0 for the input image. Our finetuning is initialized from the Stable Diffusion v1.5 checkpoint Rombach et al. (2022) to which we add additional input channels for the masked image. Since we use a pre-trained *frozen* decoder to map predicted latents back to image space, we report image quality metrics - SSIM, LPIPS, and PSNR-based solely

on the predicted diffuse texture maps. We assume that the model achieving the best performance on diffuse textures will also generalize best to the full set of PBR texture maps.

4.2 Best Model Performance

Table 1a compares our best performing model with non-finetuned SOTA baselines. Our method outperforms all baselines across all metrics. Figure 3 illustrates the model’s prediction trajectory on a validation sample throughout training. While the model successfully captures the overall structure and color distribution, it struggles to recover fine-grained texture details. These results highlight the importance of task-specific finetuning. The following subsections analyze the impact of key hyperparameters on model performance.

4.3 Guidance Scale During Inference

Diffusion models are sensitive to the guidance scale hyperparameters, which can significantly impact output quality. We evaluate the effect of varying text and image guidance scales over the grid 1.5, 2.5, 5.0, 7.5, 10.0, resulting in 25 configurations. For each, we run inference on 100 validation samples using our best model and compute standard image quality metrics. Each configuration is ranked per metric, with rank 1 denoting the best. As shown in Table 3, the best-performing setting uses a text scale

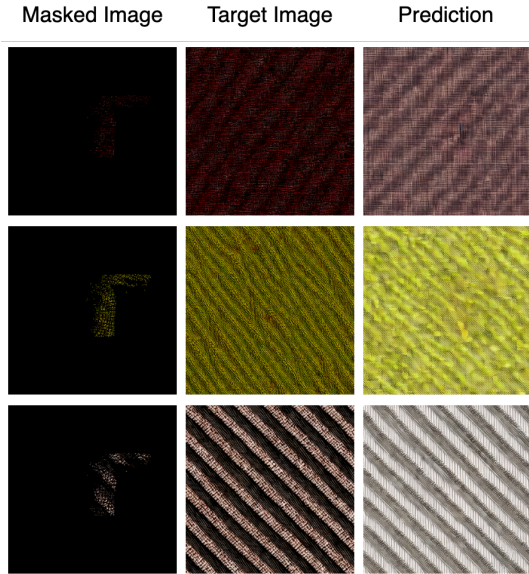


Figure 4. Hardest Cases. Hardest cases based on SSIM metric for the best model.

of 5.0 and an image scale of 2.5. However, we select the second-best configuration (text: 1.5, image: 5.0) to emphasize image guidance, which is more aligned with the task.

4.4 Training Set Size and Duration

Table 1b presents the impact of training set size and training duration on model performance. As expected, using the full dataset and training for more iterations yields the best results. However, the performance differences are relatively small—even when training on just 5,000 samples. We hypothesize that this may stem from limited diversity in the dataset, which was generated by another model, though we leave this question for future investigation.

4.5 Training Strategy and Architecture

Finetuning the full Stable Diffusion v1.5 model, which contains over one billion parameters, is computationally demanding. We therefore explore alternative strategies: finetuning only LoRA weights, training a smaller model from scratch, and initializing from an inpainting model. As shown in Table 2, full-model finetuning yields the best performance. While LoRA Hu et al. (2021) enables the use of larger batch sizes, it results in a measurable drop in quality. Training from scratch performs significantly worse, highlighting the critical role of pretraining. Surprisingly, finetuning from an in-

W	LR	Sch.	LPIPS ↓	SSIM ↑	PSNR ↑
0.50	1e-04	✗	0.45	0.16	12.41
0.75	1e-05	✗	0.58	0.14	12.21
0.25	1e-05	✗	0.63	0.12	12.08
0.50	1e-05	✓	0.69	0.12	10.70
0.50	1e-05	✗	0.69	0.09	9.88
0.00	1e-05	✗	0.78	0.06	10.07
0.50	3e-06	✗	0.83	0.09	10.22

Table 4. Comparison of Hyperparameter Configurations. The best performing configuration is highlighted in bold. For a fair comparison, all models are trained for 30 hours on 27,000 samples. Results are sorted by LPIPS, SSIM and PSNR (in that order).

painting model also underperforms. Unlike Instruct-Pix2Pix, which conditions on the masked image, noise, and text prompt, the inpainting model additionally uses the binary mask as input. Our qualitative analysis suggests that this model tends to fill only the masked garment region while leaving surrounding areas untouched, limiting its effectiveness for global texture refinement.

4.6 Optimisation Hyperparameters

Table 4 reports the impact of different hyperparameter configurations on model performance. We find that increasing the learning rate from $1e-5$ to $1e-4$ leads to the most significant improvement. Additionally, raising the DDIM loss weight from 0.50 to 0.75 yields further performance gains.

4.7 Hardest Cases

Figure 4 presents the lowest-performing cases based on SSIM for the best model. The model typically struggles with accurate color reproduction (e.g., last row) or fails to recover fine textures (e.g., middle row). We attribute this to the limited information in the masked input image, which requires the model to rely heavily on learned priors over the garment texture distribution. This is a challenging task, especially when trained on synthetic data.

4.8 Full PBR Texture Maps Prediction

During inference, the model predicts a complete set of PBR texture maps from a single masked input im-

Metric	Diffuse	Normal	Roughness	Mean
LPIPS ↓	0.45	0.26	0.28	0.33
SSIM ↑	0.17	0.50	0.52	0.40
PSNR ↑	13.04	25.76	23.63	20.81

Table 5. **Evaluation metrics for diffuse, normal, and roughness maps.** The best model’s performance on predicting a full set of PBR texture maps.

age. As illustrated in Figure 5, the predicted normal and roughness maps closely match the ground truth, while the diffuse texture exhibits noticeable deviations in color. Table 5 confirms this trend, showing stronger performance for normal and roughness prediction compared to diffuse. We attribute this discrepancy to the higher variability and ambiguity inherent in diffuse textures. Unlike normals and roughness, which are locally smooth and strongly constrained by shading cues, the diffuse map often contains high-frequency patterns and color variations that are harder to infer and continue into the masked regions.

5 Future Work & Limitations

In this work, all models were trained using the diffuse texture map as the sole supervision target in latent space. We hypothesize, however, that incorporating additional supervision from the normal and roughness maps could further enhance the model’s performance on these components. We leave this for future investigation.

Moreover, our results suggest that strong performance can be achieved with a relatively small training set, indicating that limited dataset diversity, rather than size, may be the primary bottleneck. An important avenue for future research is evaluating the model’s ability to generalize to real-world images. In this context, pretrained models such as Fabric Diffusion Zhang et al. (2024a) could be used to synthesize more realistic PBR supervision signals.

Finally, our evaluation was conducted using a single predefined mask. Future work should explore the model’s robustness to a wider range of masking patterns, including unseen or irregular occlusions.

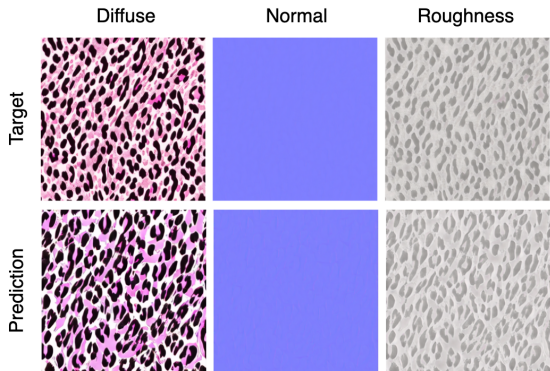


Figure 5. **Full PBR texture maps prediction.** Showcase of the best model’s prediction of a full set of PBR texture maps based on a single masked image.

6 Conclusion

We presented a method for predicting PBR texture maps from a single masked image. By fine-tuning a pre-trained Stable Diffusion v1.5 Rombach et al. (2022) on a synthetic dataset of 27,000 PBR textures, our approach produces high-quality results and outperforms state-of-the-art inpainting models that are not fine-tuned for this task. Notably, we demonstrate that comparable performance can be achieved even when training on a small subset of the dataset, and that extended training time consistently improves results.

Additionally, we find that full-model fine-tuning yields substantially better performance than using LoRA, and that fine-tuning an inpainting model underperforms compared to using the Instruct-Pix2Pix Brooks et al. (2023) pipeline.

Future work should investigate the model’s generalization to real-world images and explore the benefits of incorporating additional supervision from normal and roughness maps to enhance performance on these texture components. Another promising direction is studying the role of the mask in shaping the model’s effectiveness and robustness.

7 Acknowledgements

I would like to thank my supervisor, Yingxuan You, for her valuable feedback and guidance throughout the semester. Further, I would like to thank Prof. Fua for hosting me in his lab and providing me with the computational resources that made this work

possible.

References

- Tim Brooks, Aleksander Holynski, and Alexei A. Efros. Instructpix2pix: Learning to follow image editing instructions, 2023. URL <https://arxiv.org/abs/2211.09800>.
- Kai He, Kaixin Yao, Qixuan Zhang, Jingyi Yu, Lingjie Liu, and Lan Xu. Dresscode: Autoregressively sewing and generating garments from text guidance. *ACM Transactions on Graphics (TOG)*, 43(4):1–13, 2024.
- Zijian He, Yuwei Ning, Yipeng Qin, Guangrun Wang, Sibei Yang, Liang Lin, and Guanbin Li. VTON 360: High-fidelity virtual try-on from any viewing direction. In *Proceedings of the IEEE/CVF Conference on Computer Vision and Pattern Recognition (CVPR)*, 2025.
- Jonathan Ho and Tim Salimans. Classifier-free diffusion guidance, 2022. URL <https://arxiv.org/abs/2207.12598>.
- Edward J. Hu, Yelong Shen, Phillip Wallis, Zeyuan Allen-Zhu, Yuanzhi Li, Shean Wang, Lu Wang, and Weizhu Chen. Lora: Low-rank adaptation of large language models, 2021. URL <https://arxiv.org/abs/2106.09685>.
- Diederik P Kingma and Max Welling. Auto-encoding variational bayes, 2022. URL <https://arxiv.org/abs/1312.6114>.
- Hyun-Song Kwon and Sung-Hee Lee. Deepiron: Predicting unwarped garment texture from a single image, 2023. URL <https://arxiv.org/abs/2310.15447>.
- Luping Liu, Yi Ren, Zhijie Lin, and Zhou Zhao. Pseudo numerical methods for diffusion models on manifolds, 2022. URL <https://arxiv.org/abs/2202.09778>.
- Ivan Lopes, Fabio Pizzati, and Raoul de Charette. Material palette: Extraction of materials from a single image. In *CVPR*, 2024.
- Shuliang Ning, Duomin Wang, Yipeng Qin, Zirong Jin, Baoyuan Wang, and Xiaoguang Han. Picture: Photorealistic virtual try-on from unconstrained designs. In *Proceedings of the IEEE/CVF Conference on Computer Vision and Pattern Recognition (CVPR)*, pages 6976–6985, June 2024.

- Alec Radford, Jong Wook Kim, Chris Hallacy, Aditya Ramesh, Gabriel Goh, Sandhini Agarwal, Girish Sastry, Amanda Askell, Pamela Mishkin, Jack Clark, Gretchen Krueger, and Ilya Sutskever. Learning transferable visual models from natural language supervision, 2021. URL <https://arxiv.org/abs/2103.00020>.
- Robin Rombach, Andreas Blattmann, Dominik Lorenz, Patrick Esser, and Björn Ommer. High-resolution image synthesis with latent diffusion models, 2022. URL <https://arxiv.org/abs/2112.10752>.
- Nikolaos Sarafianos, Tuur Stuyck, Xiaoyu Xiang, Yilei Li, Jovan Popovic, and Rakesh Ranjan. Garment3dgen: 3d garment stylization and texture generation, 2025. URL <https://arxiv.org/abs/2403.18816>.
- Sam Sartor and Pieter Peers. Matfusion: a generative diffusion model for svbrdf capture. In *ACM SIGGRAPH Asia Conference Proceedings*, December 2023.
- Jiaming Song, Chenlin Meng, and Stefano Ermon. Denoising diffusion implicit models, 2022. URL <https://arxiv.org/abs/2010.02502>.
- Astitva Srivastava, Pranav Manu, Amit Raj, Varun Jampani, and Avinash Sharma. Wardrobe: Text-guided generation of textured 3d garments, 2024. URL <https://arxiv.org/abs/2403.17541>.
- Linxuan Xin, Zheng Zhang, Jinfu Wei, Wei Gao, and Duan Gao. Dreampbr: Text-driven generation of high-resolution svbrdf with multi-modal guidance, 2024. URL <https://arxiv.org/abs/2404.14676>.
- Xin Yu, Ze Yuan, Yuan-Chen Guo, Ying-Tian Liu, Jianhui Liu, Yangguang Li, Yan-Pei Cao, Ding Liang, and Xiaojuan Qi. Texgen: a generative diffusion model for mesh textures. *ACM Trans. Graph.*, 43(6), 2024. ISSN 0730-0301. doi: 10.1145/3687909.
- Cheng Zhang, Yuanhao Wang, Francisco Vicente Carrasco, Chenglei Wu, Jinlong Yang, Thabo Beeler, and Fernando De la Torre. FabricDiffusion: High-fidelity texture transfer for 3d garments generation from in-the-wild images. In *ACM SIGGRAPH Asia*, 2024a.
- Yuqing Zhang, Yuan Liu, Zhiyu Xie, Lei Yang, Zhongyuan Liu, Mengzhou Yang, Runze Zhang, Qilong Kou, Cheng Lin, Wenping Wang, and Xiaogang Jin. Dreammat: High-quality pbr material generation with geometry- and light-aware diffusion models. *ACM Trans. Graph.*, 43(4), jul 2024b. ISSN 0730-0301. doi: 10.1145/3658170. URL <https://doi.org/10.1145/3658170>.
- Jiali Zheng, Rolando Alexopoulos Potamias, and Stefanos Zafeiriou. Design2cloth: 3d cloth generation from 2d masks. In *Proceedings of the IEEE/CVF Conference on Computer Vision and Pattern Recognition (CVPR)*, pages 1748–1758, June 2024.